Pol. J. Environ. Stud. Vol. 35, No. 4 (2026), 4667-4676
DOI: *10.15244/pjoes/207485* ONLINE PUBLICATION DATE: 2025-09-15

Original Research

Efficient Removal of Polyethylene Using Magnesium Hydroxide and Anionic Polyacrylamide as Dual-Coagulant by Coagulation-Flocculation Processes

Xinge Li, Bo Li, Jianhai Zhao*, Hongying Yuan, Yongzhi Chi

Tianjin Key Laboratory of Aquatic Science and Technology, School of Environmental and Municipal Engineering, Tianjin Chengjian University, 26 Jinjing Road, Xiqing District, Tianjin, 300384, China

Received: 17 January 2025
Accepted: 24 June 2025

Abstract

Microplastics, a new type of contamination, were extensively distributed in water areas with increasing plastic production and poor management of plastic waste. Simultaneously, removing pollutants from water was a popular research topic in the field of water treatment. In this investigation of water treatment, simulated natural water containing polyethylene was treated using magnesium hydroxide and anionic polyacrylamide as dual coagulants. Based on a series of experiments, the optimum reactor conditions were an Mg^{2+} concentration of 40 mg/L, a pH of 12, and a temperature of 20°C. The maximum removal efficiency of polyethylene could reach 84.9% ± 3% under the optimal experimental conditions with the average size of flocs 57.19 μm. Using an intelligent Photometric Dispersion Analyzer, the full processes of coagulation-flocculation were recorded. Evaluating coagulation-flocculation performance using flocs' flocculation index and polyethylene removal efficiency as metrics. Scanning electron microscopy, Fourier transform infrared spectroscopy, and zeta potential were used to study the performance and coagulation characteristics. The results of this work confirm that the removal of microplastics relied on adsorption bridge and sweep flocculation mechanisms. This study provides a valuable theoretical basis for an in-depth comprehension of the performance and coagulation characteristics of removing polyethylene from wastewater.

Keywords: magnesium hydroxide, anionic polyacrylamide, microplastics, polyethylene, coagulation-flocculation

*e-mail: jhzhao@tcu.edu.cn

© 2026 This article is licensed under a Creative Commons Attribution-NonCommercial 4.0 International (CC BY-NC 4.0)

Table 1. Comparison of novel microplastic removal processes among different studies.

Methods	Material	Advantages	Drawbacks	Reference
Sorption	Algae (spirulina)	Green, no pollution, biodegradability, minimal toxicity	Nonrecyclable	[22]
Membrane technology	Membrane bioreactor	High removal efficiency	Membrane fouling	[23]
Membrane technology	Forward osmosis membranes	Excellent fouling resistance against microplastics, nonchemical treatment	High treatment costs	[24]
Ingestion	Fish	Large-scale application	Low applicability, lack of reproducibility	[25]
Biological degradation	Enzyme	Simplicity and safety	Low removal efficiency	[26]
Electrocoagulation	Aluminum electrodes	High removal efficiency, not relying on chemicals or microorganisms	Energy demand, high cost	[27]
Photocatalytic degradation	TiO_2	Environmentally friendly	Low removal efficiency	[28]
Coagulation	PS-PAM	Simple mechanical devices, low capital cost, simple operation	Addition of chemicals, nonusable for large microplastics	[29]

Introduction

Microplastics (MPs), as an emerging kind of potentially threatening contamination, have been drawing more attention as an emerging contaminant due to their stable structure, low biodegradability, and easy accumulation since the term was first put forward in 2004 [1, 2]. MPs were characterized as plastic fragments and particles smaller than 5 mm in diameter, which was consistent with previous results that large plastics fragment into smaller pieces through mechanical effects, photooxidation, and biodegradation [3-5]. Based on their sources, MPs were usually categorized into two categories, namely primary microplastics and secondary microplastics [6, 7]. Primary MPs were raw materials used in personal care and cosmetic products (PCCPs), such as eye shadows, blush powders, makeup foundations, shower gels, shampoos, and creams [8]. Secondary MPs originate from the environmental degradation of raw plastic particles through physical, chemical, and biological processes [9]. Examples of secondary microplastics were microfibers from textiles, tire dust from vehicles, and fragments of agricultural plastics [10]. MPs' products were widely used in daily life, bringing convenience while generating environmental pollution [11]. Due to extensive usage and increasing production of plastic products, research on the prevalence of MPs and their potential negative impacts on various ecosystems is currently thriving.

In recent decades, MPs have been widely found in various environmental mediums such as the atmosphere, soils, seawater, freshwater, and even human breast milk [12-16]. Due to the omnipresence of MPs in the environment, human exposure is unavoidable, occurring mainly through three pathways: ingestion, inhalation, and dermal contact [17]. Among all of them, ingestion was deemed the primary pathway. In addition, the small particle size, extensive specific surface area, and substantial volume ratio of MPs facilitate the adsorption of numerous contaminants. Antibiotics, heavy metals, and persistent organic pollutants can also be adsorbed to microplastics, which can accelerate the toxicity in aquatic organisms through the food chain, thereby affecting human health [18-20]. In general, MPs could cause cytotoxicity, obesity, and infertility and increase the risk of chronic inflammation, cancer, and neurodegenerative and immune diseases in humans. MPs' widespread presence and un-environmental friendliness affirmed the need for research to minimize their discharge into the environment.

In the past decades, many strategies have been tried to degrade the MPs from water, including physical sorption and filtration, biological removal and ingestion, and chemical treatments [21]. Adsorption and membrane technology were the main physical adsorption and filtration methods. The adsorption of microplastics on the surface of green algae was heavily influenced by the surface charge of the particles [22]. With high removal efficiency, membrane technology could be applied to the treatment of microplastics in most aqueous environments [23, 24]. However, treatment costs were also higher and associated with high pollution levels. Microbiological techniques, such as ingestion and microplastic removal by organisms, show potential for large-scale application [25, 26]. However, the applicability in different water environments needs to be further studied owing to the complexity of the water quality background of water bodies. The chemical treatments mainly include electrocoagulation, photocatalytic degradation, and classic coagulation [27-29]. The coagulation-flocculation method was extensively applicable to wastewater treatment because of controllable operational conditions,

simple mechanical devices, low capital cost, and simple operation. Compared with the above pathways for degrading MPs, as shown in Table 1, the method of coagulation-flocculation exhibited predominant potential for degrading MPs.

Different kinds of MPs, including polyethylene terephthalate, polyurethane, polystyrene, polyvinyl chloride, polypropylene, polyesters, polyethylene (PE), and polyamide, have been identified in water [17, 30, 31]. Nevertheless, the percentage of PE is significantly greater than that of other MPs [32]. PE is widely utilized across various sectors and is the primary constituent of MPs, which are waste in aquatic environments. In addition, PE particles exhibited poor solubility in water, with a density slightly less than that of water, which was easily suspended in water. As a result, the primary purpose of this study was to combine magnesium hydroxide ($Mg(OH)_2$) and anionic polyacrylamide (PAM) to remove PE, chiefly to understand the influences of dosage of Mg^{2+}, initial pH, and temperature on removal efficiency. $Mg(OH)_2$ is an affordable and eco-friendly chemical that quickly forms precipitates and could rapidly attract negatively charged colloidal flocs in alkaline wastewater due to its positive surface charge [33, 34]. When treating water and wastewater, anionic PAM is usually applied as a coagulant to enhance flocculation, facilitating the formation of large aggregates by bridging destabilized particles, which have good settling properties [19, 35]. As a result, this system used $Mg(OH)_2$ and anionic PAM, which are widely used in sewage disposal as coagulants. In addition, coagulation and flocculation, the method used in this experiment, has the advantages of controlled operating conditions, simple mechanical devices, low capital costs, and simple operation. In conclusion, using anionic PAM with $Mg(OH)_2$ was a cost-effective and efficient method for removing PE due to flocs' quick formation and growth through dual-coagulant coagulation and flocculation. The removal performance and characteristics of PE by $Mg(OH)_2$ and anionic PAM dual-coagulant were also systematically studied.

Materials and Methods

Materials and Chemicals

All chemicals involved were of at least analytical grade (AR). $MgCl_2 \cdot 6H_2O$ and anionic PAM were bought from Guangfu Fine Chemical Research Institute Co., located in Tianjin, China. Humic acid, kaolin, and PE were purchased from Jiangtian Technology Co., located in Tianjin, China. Sodium hydroxide (NaOH) and hydrochloric acid (HCl) were purchased from Kewei Co., located in Tianjin, China. All the chemicals employed were used without further purification.

Apparatus and Characterization

An online intelligent Particle Dispersion Analyzer (iPDA) (PDA2000, Econovel, Korea) was used to measure the Flocculation Index (FI) and the size distribution of flocs. Zeta potential was measured by Malvern Zetasizer Nano ZS (Malvern, UK). Fourier transform infrared (FT-IR) spectra (4000-1500 cm^{-1}) were recorded by an NI Nicolet iS 10 FT-IR Spectrometer (NICOLET, USA). Measurements of floc size distribution were conducted with the Mastersizer 2000 by Malvern, UK, and floc images were obtained using the IX71 digital photomicrography from Olympus, Japan. Images were obtained using Scanning Electron Microscopy (SEM) with a Quanta 200 from FEI, Czech.

Preparation of Simulated Natural Water

Simulated natural water was produced by adding 0.20 g of kaolin and 0.12 g of humic acid into 10.00 L of deionized water to provide concentrations of 20 mg/L of kaolin and 12 mg/L of humic acid, stirring for 12 h at a constant speed to mix well and fully dissolve. The application of kaolin and humic acid was to replicate actual water's turbidity and natural organic content. After mixing, the pH was altered to 12 by 1 M NaOH and HCl solution. The pH of the solution was strictly controlled at 12 to ensure that a large amount of $Mg(OH)_2$ was prepared. The simulated PE plastic water samples were prepared by adding 0.05 g of PE into 1 L of the simulated natural water. Samples were pre-washed with 1 M of HCl to remove residues before the coagulation experiment. The stock solution should be kept in a dark environment at 4°C.

Coagulation Experiments with Jar Tests

Batch coagulation experiments were conducted in a six-mixer jar-test setup with 1-L beakers at 20 ± 1°C. Simulated water was added to a 1-L beaker and stirred at 300 rpm for 2 minutes. The stirring speed was reduced to 60 rpm for 5 minutes, followed by 5 minutes of sedimentation. After 30 seconds of rapid stirring, 10 - 50 mg/L of magnesium ions were mixed, and 5 mg/L of anionic PAM was introduced 10 seconds before the stirring ended. Anionic PAM is a kind of polymer flocculant, and as a coagulant, it aids in the coagulation process, which can improve the coagulation performance. Following coagulation and precipitation, the zeta potential was assessed by taking samples from the supernatant at a height of 3 cm, and the characteristics of the flocs with adsorbed PE were gathered for analysis. An online iPDA was employed to monitor the Flocculation Index (FI) during the coagulation phase. Three parallel experiments were conducted for each jar test to ensure the experiment's repeatability and the data's credibility.

Removal Efficiency of Polyethylene

As of today, there is no standardized quantitative method for MPs. Weighing was an accurate method among the existing ones [19, 35]. To determine the removal efficiency of PE, the weighing method was chosen, involving the measurement of quality change pre- and post-coagulation experiments. The specific procedures of sample preparation were as follows:

Before the coagulation experiments, an analytical balance (1.0×10^{-4} g) was utilized to accurately measure a specific amount of PE particle, with an initial PE concentration of 50 mg/L. Following the coagulation tests, the surface-floating PE particles were collected using a 25.0 mL syringe, washed three times with HCl to eliminate impurities, and then filtered using a 0.45 μm membrane vacuum filter pump. It was remarkable that, before and after the coagulation experiments, air-drying at 60°C, the PE particles were dried for 12 hours until their weight did not change. Each experiment was repeated three times. The removal efficiency (η) can be calculated from the weight of PE M_0 and M_1.

$$\eta\% = \frac{M_0 - M_1}{M_0} \times 100 \quad (1)$$

M_0 represented the initial weight of PE placed in each beaker prior to starting the coagulation experiment, and M_1 was the weight of PE that remained floating on the water post-coagulation.

Results and Discussion

Effects of Experimental Conditions on the Removal Efficiency of Microplastics

Effects of Different Dosages of Mg^{2+} on Removal Efficiency

To explore the optimal dosage of Mg^{2+} during coagulation, a 10-50 mg/L combined dose of Mg^{2+} and anionic PAM (5 mg/L) was conducted, respectively. Fig. 1a) demonstrates that the peak FI value of 7.2 was achieved with a Mg^{2+} concentration of 40 mg/L, leading to large aggregated flocs forming. Upon increasing the Mg^{2+} dose to 50 mg/L, the FI value of the flocs fluctuated in the high range of 2.5-4.5, still showing a good trend of FI value change. In addition, as shown in Fig. 1b), the removal efficiency of PE also initially increased when the dose of Mg^{2+} was in the range of 10-40 mg/L; the removal rates were 45.97%, 57.36%, 63.37%, and 84.90%, respectively. While the Mg^{2+} dosage was 50 mg/L, the removal rate decreased significantly to about 60%, which indicates that increasing the dosage of Mg^{2+} after reaching the optimal dosage has the opposite effect on the overall coagulation effect. It was presumed that as the concentration of Mg^{2+} increased, a large number of positively charged colloids were generated in the solution. The generation of a large number of positively charged colloids increased the electrostatic repulsion between the colloids, which resulted in poor agglomeration between the flocs. As shown in Fig. 1b), the zeta potential values were -38.60 mV, -30.20 mV, -26.50 mV, and -22.60 mV at 10-40 mg/L Mg^{2+} dosages. The zeta potential in the solution increased uniformly with the concentration gradient of Mg^{2+}, which further corroborated that 40 mg/L of Mg^{2+} was the optimum dosage. On balance, a 40 mg/L Mg^{2+} concentration was the best dosage in this work.

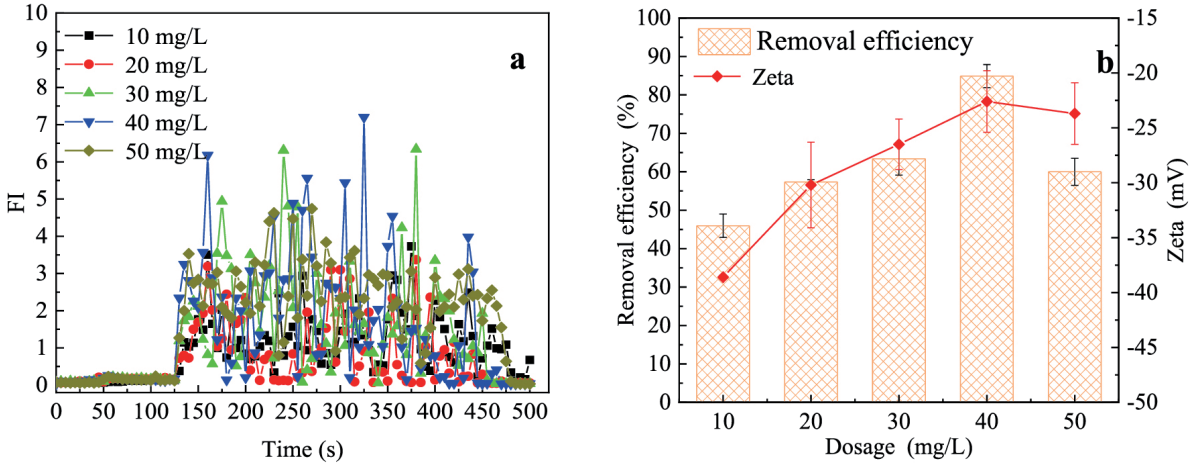

Fig. 1. a) Effect of Mg^{2+} dosage on FI. b) Effect of Mg^{2+} dosage on removal efficiency.

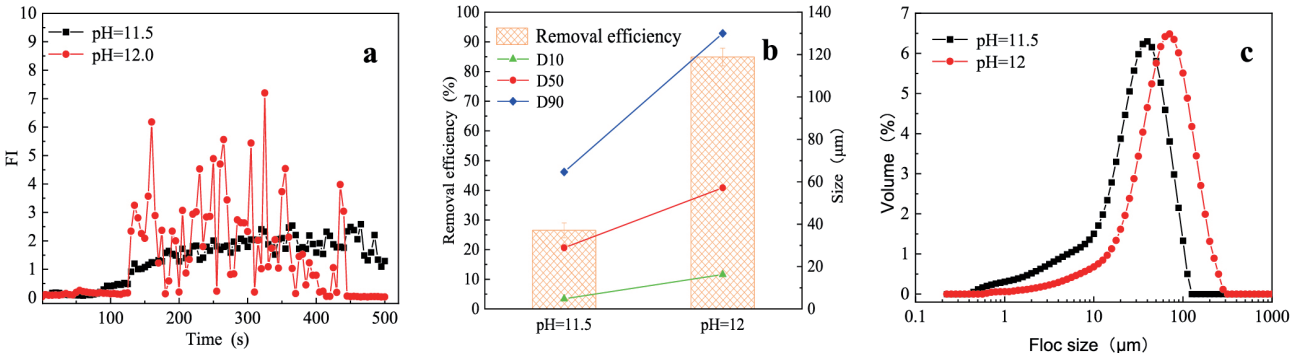

Fig. 2. a) Effect of pH on FI. b) Effect of pH on removal efficiency. c) Effect of pH on the particle size distribution of flocs.

Effects of the Initial pH on Removal Efficiency

The pH of the solution can serve as a vital parameter in the choice of the $Mg(OH)_2$ and anionic PAM coagulation technology. When the appropriate amount of Mg^{2+} was added, the amount of generated $Mg(OH)_2$ depended on the amount of hydroxide ions. At low pH, a sufficient amount of $Mg(OH)_2$ could not be formed, thus affecting the nucleation of $Mg(OH)_2$ and the adsorption of humic acid and kaolin, which resulted in the particle size of the flocculent material generating relatively small during the coagulation process. When the pH was higher, the generated $Mg(OH)_2$ precipitates in a colloidal state, which could be used as an efficient coagulant [36-38].

To investigate the effects of pH on coagulation performance in this work, the pH of the simulated water was adjusted from 11.5 to 12. Fig. 2a) shows the effect of the initial pH on removal efficiency under pH of 11.5 and 12 at temperatures of 20°C. The FI values of the flocs were always about 2.0 during the whole process of coagulation at pH 11.5. This suggested that floc particle sizes were relatively small under these conditions. However, at pH 12, the sizes of floc particles gradually increased with time during the slow churning stage. The average FI at pH 12 was higher than that at pH 11.5. This indicated that the amount of hydroxide in the wastewater was reflected by pH, and when the optimal amount of Mg^{2+} was added, the amount of generated $Mg(OH)_2$ depended on the amount of hydroxide. Consequently, the relatively low pH value was unsuitable for forming enough $Mg(OH)_2$. This affects the nucleation of $Mg(OH)_2$ and the adsorption of PE, so the floc size produced in the coagulation process was relatively small.

A significant relationship was observed between floc size during coagulation and the effectiveness of PE removal. D10, D50, and D90 represented the particle size distribution of coagulants at 10%, 50%, and 90% of their diameters, respectively. D50 was defined as the median diameter. The particle size varied significantly between the two conditions, with D10, D50, and D90 being 4.8 μm, 28.9 μm, and 64.6 μm at pH 11.5, and 16.3 μm, 57.2 μm, and 130.0 μm, respectively, at pH 12. In addition, Fig. 2b) depicts the PE removal efficiency and the average floc size throughout the coagulation process. At a lower pH of 11.5, the removal efficiency of PE was just 26.51 ± 2.5%, indicating that larger particle sizes may improve PE removal efficiency by facilitating the formation of larger flocs with the coagulant. As mentioned above, the results of the FI value and the lower pH value limited the amount of $Mg(OH)_2$ production, resulting in smaller floc particle size during the whole coagulation process, thus seriously affecting the removal of PE.

Based on the above experimental results, the influence of pH on the growth effect of flocs was explored, and the flocs generated under the two conditions were analyzed by a laser particle size analyzer, respectively. As shown in Fig. 2c), the median particle size at pH 11.5 was 28.9 μm, which was half the median particle size at pH 12. Furthermore, flocs with particle sizes larger than 100 μm were almost nonexistent at pH 11.5, which explains the low FI of flocs and PE removal efficiency.

Effects of Temperature on Removal Efficiency

Besides dosages of Mg^{2+} and pH, the influence of the temperature of the solution was also a factor that needed to be investigated. The solution temperature affects the floc growth by influencing the viscosity of water and the chemical reaction of $Mg(OH)_2$ flocs on the one hand and the PE removal efficiency by influencing the adsorption bridging effect of anionic PAM on the other hand. As the temperature rises, the viscosity of water decreases, the resistance to particle movement decreases, and floc aggregation accelerates. In addition, the $Mg(OH)_2$ flocs were generated by hydrolysis and became progressively larger as the temperature increased. However, the floc structure becomes fragile and susceptible to shear damage above the appropriate temperature. Furthermore, the adsorption bridge and sweep flocculation of anionic PAM can be promoted by appropriately increasing the temperature.

As shown in Fig. 3a), at the temperature of the solution at 15°C, the FI values were lower than at other temperatures, which indicates that the lower temperatures had an inhibitory effect on the coagulation reaction and were unfavorable for floc growth. At 20°C

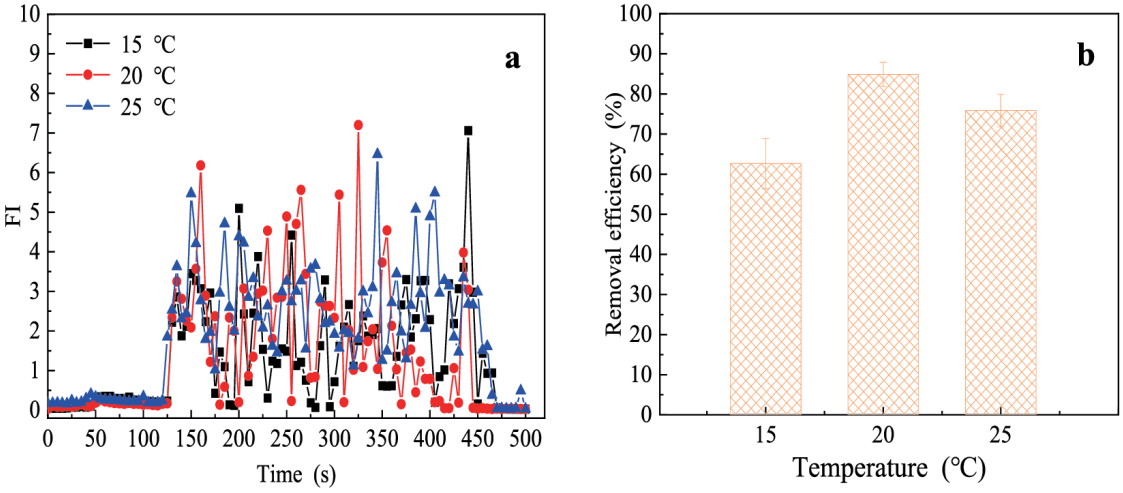

Fig. 3. a) Effect of different temperature conditions on FI. b) Effect of temperature on removal efficiency.

and 25°C temperatures, the FI values were in the range of 1.5-3.5 with minor differences. However, compared with FI values under the two types of conditions, at the range of FI values greater than 3.5, the maximum values were 7.2 and 6.8, respectively. It can be found that the low-temperature environmental conditions were not conducive to the coagulation reaction. As shown in Fig. 3b), the PE removal efficiency was influenced by different solution temperatures. The removal efficiencies obtained at the temperatures of 15°C, 20°C, and 25°C were 62.66 ± 6.28%, 84.9 ± 3%, and 75.86 ± 4.03%, respectively. This indicated that at the water temperature of 20°C, the coagulation effect was better and more suitable for the floc growth in the coagulation process of this experiment.

As shown in Fig. 4a), the agglomerated flocs were generated under different temperature conditions. In comparison, when the solution temperature was at 15°C, the flocs were loosely agglomerated, and the PE particles embedded on the surface were fewer; as a result, the removal rate of PE was relatively low. When the solution temperature was 20°C, as shown in Fig. 4b), the combination between the flocs was very dense, and the color was further deepened. At the same time, a large number of PE particles were tightly wrapped inside the flocs via adsorption bridge and sweep flocculation. The removal of PE was optimally achieved under these conditions. While the temperature of the solution was 25°C, as shown in Fig. 4c), it was visible that the PE particles on the flocs' surface and the tightness of flocs agglomeration were slightly decreased. The removal efficiency of PE at 25°C was lower than that at 20°C. Combined with the above experimental results, the optimal effect of PE removal was achieved at 20°C, clearly illustrating the effectiveness of temperature on PE removal.

Flocs Characteristics

In order to more accurately illustrate the influence of Mg^{2+} dosage on the agglomeration effect of flocs, SEM of floc particles was made separately with the Mg^{2+} dosage in the range of 10-50 mg/L. As seen in Fig. 5, the agglomeration effect of flocs becomes more obvious with the increase in Mg^{2+} usage. When 10 mg/L of Mg^{2+} was added, the vast majority of the floc surface area was smooth and loose, spread with independently distributed small particles, and the adsorption capacity of this structure was weak, indicating that it was not easy to form large-size flocs under these conditions. When the Mg^{2+} dose was 20 mg/L or 30 mg/L, the morphology of flocs changed. When the Mg^{2+} dosage was increased

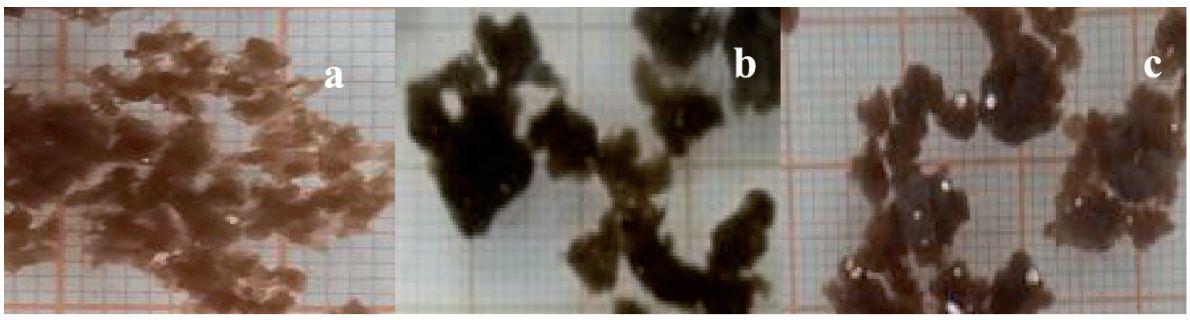

Fig. 4. The floc aggregation at different temperature conditions. a) 15°C, b) 20°C, c) 25°C.

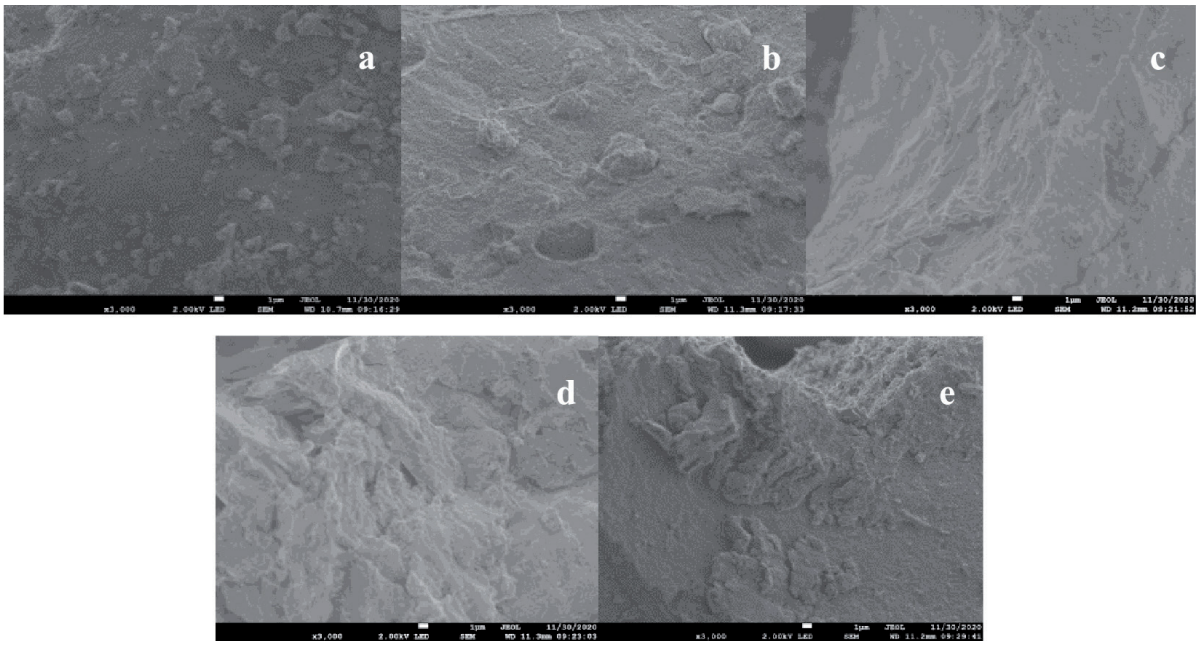

Fig. 5. Flocs image of flocs with different Mg^{2+} dosages. a) 10 mg/L, b) 20 mg/L, c) 30 mg/L, d) 40 mg/L, e) 50 mg/L.

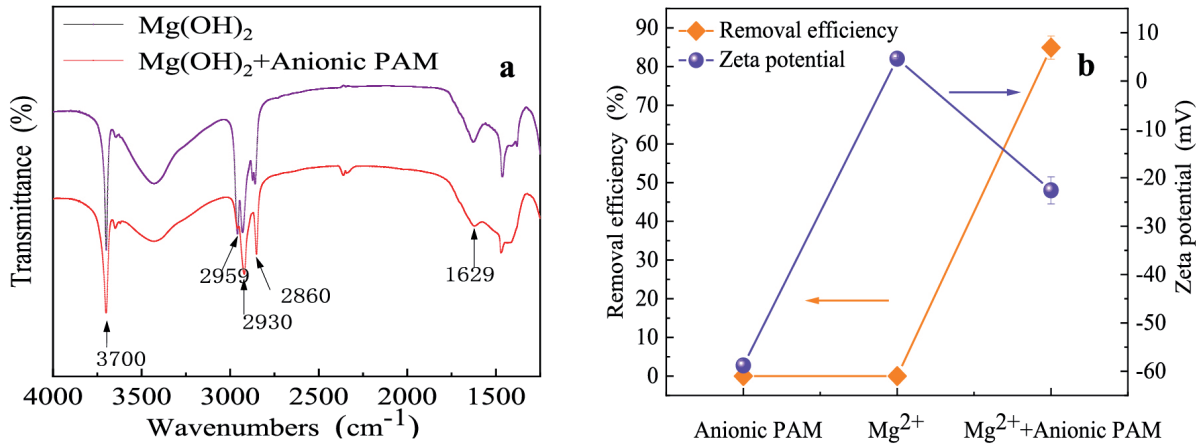

Fig. 6. a) IR spectra of coagulation flocs. b) Removal efficiency and zeta potential of different coagulant types.

to 40 mg/L, the agglomeration effect was obvious; the floc surface appeared to be a dense and irregular blocky structure, which was due to the formation of enough $Mg(OH)_2$. Under the action of the strong adsorption bridge of anionic PAM, the flocs are wrapped together layer by layer. It was assumed that the low concentration of Mg^{2+} in the early stage could not generate sufficient $Mg(OH)_2$ coagulant. When the amount of Mg^{2+} was increased, a large amount of $Mg(OH)_2$ coagulant was generated, which adsorbed the pollutants in the solution through electrical neutralization, thus generating numerous small flocs. Therefore, the flocs were able to agglomerate well through the bridging effect of PAM to achieve the purpose of efficiently removing the PE. With the Mg^{2+} amount further boosted to 50 mg/L, the agglomeration effect was not as good as the condition of 40 mg/L Mg^{2+}. In addition, the amount of Mg^{2+} used has a certain influence on the floc properties and the agglomeration effect, which was more favorable to removing PE.

The FT-IR was used to analyze the chemical bonds of flocs to further understand their characteristics. According to Fig. 6, the FT-IR spectra were presented for both $Mg(OH)_2$ flocs and the dual coagulant flocs consisting of $Mg(OH)_2$ and anionic PAM. The strong and broad peak near 3700 cm^{-1} could be due to the stretching vibration of hydroxyl groups. The absorption peak at 1629 cm^{-1} could be due to the bending vibration of Mg-OH. In addition, the absorption peak at 2959 cm^{-1} could be attributed to the antisymmetric stretching vibration of the saturated alkane CH_3. The CH_2 vibrations that involve asymmetric and symmetric stretching were responsible for the absorption peaks at 2930 cm^{-1} and 2860 cm^{-1}, respectively. In conclusion, the 3700 cm^{-1}

and 1629 cm^{-1} infrared spectra indicate that the product was $Mg(OH)_2$, whereas anionic PAM was only adsorbed on the $Mg(OH)_2$ surface without chemisorption. This indicated that the adsorption was a physical process, as no covalent bonds were formed during the adsorption. In addition, FT-IR characterization could confirm that adsorption bridging and sweeping served as the primary mechanisms in this study's coagulation and flocculation process, as established in several studies [39, 40].

It is well known that the process of charge neutralization and flocculation formation is related to the change of zeta potential. The hydrolysates of Mg^{2+} as the positively charged core could be easily adsorbed on the surface of the negatively charged particles, destabilizing the particles. The zeta potential in Fig. 6b was -58.8 mV with only anionic PAM, close to the original solution's -57.3 mV, implying no coagulation reaction occurred. The results are consistent with the efficiency of removing PE being approximately zero. In addition, the zeta potential significantly increased from -58.8 mV to 4.62 mV with the exclusive use of magnesium ions. The above results were the same as the previous study [41]. The efficiency of removing PE from wastewater was nearly nonexistent. Upon analysis, it was found that the flocs formed were too small to effectively remove PE when only Mg^{2+} was used during coagulation. According to previous studies, removing pollutants using $Mg(OH)_2$ coagulation was largely due to charge neutralization and adsorption. When appropriate amounts of Mg^{2+} and anionic PAM were compounded, the zeta potential of the solution was dropped to -22.6 mV. At the same time, the removal of PE with removal efficiency plummeted to 84.9 ± 3%. The presumption was that a vast majority of the PE was encapsulated in the large flocs formed by the bridging and sweeping of the PAM and eventually settled with the flocs.

In summary, based on the study of SEM, zeta potential, and characteristics of flocs, the performance and coagulation characteristics were favorable in dual-coagulation systems. In addition, the results of this work confirm that the removal of microplastics relied on adsorption bridge and sweep flocculation mechanisms. The mechanism of the coagulation process was not singular. The dominant mechanisms were bridging and sweeping through adsorption when using $Mg(OH)_2$ and anionic PAM as dual coagulants to treat wastewater. Different mechanisms may play a dominant role in different systems.

Conclusions

In summary, we developed a dual-coagulation system for improving the coagulation performance and floc characteristics of a combination of $Mg(OH)_2$ and anionic PAM in this study. For the range of parameters investigated, the optimum reactor conditions were found to be Mg^{2+} concentration 40 mg/L, pH 12, and temperature 20℃, which can improve the removal efficiency of PE. During the rapid mixing period, the formation of flocs depends on the precipitation of $Mg(OH)_2$, and the bridging function of anionic PAM aided their growth. In addition, this study's coagulation-flocculation mechanism was researched using zeta potential and FTIR analysis. The main mechanisms of the composite system were adsorption bridge and sweep flocculation. This study, which could provide an important theoretical basis for the characteristics and mechanisms of coagulation technology to remove polyethylene, is highly important for addressing PE in wastewater.

Acknowledgments

This research was funded by the Technology Research and Development Program of Tianjin, grant number 22YFXTHZ00080, and partly by the National Key Research and Development Project IV, "Ecological environment and geological effect evaluation of in-situ mining of oil shale" of the National Oil Shale Ecological Environment Subcenter, grant number 2019YFA0705504.

Conflict of Interest

The authors declare no conflict of interest.

References

1. THOMPSON R.C., OLSEN Y., MITCHELL R.P., DAVIS A., ROWLAND S.J., JOHN A.W., MCGONIGLE D., RUSSELL A.E. Lost at sea: where is all the plastic? SCIENCE. **304** (5672), 838, **2004**.
2. SHAO Y., HUA X., LI Y., WANG D. Comparison of reproductive toxicity between pristine and aged polylactic acid microplastics in Caenorhabditis elegans. Journal of Hazardous Materials. **466**, 133545, **2024**.
3. LI C., BUSQUETS R., CAMPOS L.C. Assessment of microplastics in freshwater systems: A review. Science of the Total Environment. **707**, 135578, **2020**.
4. FAN L., MOHSENI A., SCHMIDT J., EVANS B., MURDOCH B., GAO L. Efficiency of lagoon-based municipal wastewater treatment in removing microplastics. Science of the Total Environment. **876**, 162714, **2023**.
5. SUN A., WANG W.X. Reducing Gut Dissolution of Zinc Oxide Nanoparticles by Secondary Microplastics with Consequent Impacts on Barnacle Larvae. Environmental Science & Technology. **58** (3), 1484, **2024**.
6. AHMED A.S.S., BILLAH M.M., ALI M.M., BHUIYAN M.K.A., GUO L., MOHINUZZAMAN M., HOSSAIN M.B., RAHMAN M.S., ISLAM M.S., YAN M., CAI W. Microplastics in aquatic environments: A comprehensive review of toxicity, removal, and remediation strategies. Science of the Total Environment. **876**, 162414, **2023**.
7. KYE H., KIM J., JU S., LEE J., LIM C., YOON Y. Microplastics in water systems: A review of their impacts

on the environment and their potential hazards. Heliyon. **9** (3), e14359, **2023**.
8. KABIR M.S., WANG H., LUSTER-TEASLEY S., ZHANG L., ZHAO R. Microplastics in landfill leachate: Sources, detection, occurrence, and removal. Environmental Science and Ecotechnology. **16**, 100256, **2023**.
9. TAKEUCHI H., TANAKA S., KOYUNCU C.Z., NAKADA N. Removal of microplastics in wastewater by ceramic microfiltration. Journal of Water Process Engineering. **54**, 104010, **2023**.
10. M RAHIM N.A.S., ISLAHUDIN F., ABU TAHRIM N., JASAMAI M. Microplastics in Cosmetics and Personal Care Products: Impacts on Aquatic Life and Rodents with Potential Alternatives. Sains Malaysiana. **51** (8), 2495, **2021**.
11. LI S., YANG Y., YANG S., ZHENG H., ZHENG Y., M J., NAGARAJAN D., VARJANI S., CHANG J.S. Recent advances in biodegradation of emerging contaminants - microplastics (MPs): Feasibility, mechanism, and future prospects. Chemosphere. **331**, 138776, **2023**.
12. RAGUSA A., NOTARSTEFANO V., SVELATO A., BELLONI A., GIOACCHINI G., BLONDEEL C., ZUCCHELLI E., DE LUCA C., D'AVINO S., GULOTTA A., CARNEVALI O., GIORGINI E. Raman Microspectroscopy Detection and Characterisation of Microplastics in Human Breastmilk. Polymers (Basel). **14** (13), 2700, **2022**.
13. ABBASI S., KESHAVARZI B., MOORE F., TURNER A., KELLY F.J., DOMINGUEZ A.O., JAAFARZADEH N. Distribution and potential health impacts of microplastics and microrubbers in air and street dusts from Asaluyeh County, Iran. Environmental Pollution. **244**, 153, **2019**.
14. GUO J.J., HUANG X.P., XIANG L., WANG Y.Z., LI Y.W., LI H., CAI Q.Y., MO C.H., WONG M.H. Source, migration and toxicology of microplastics in soil. Environment International. **137**, 105263, **2020**.
15. WANG S., CHEN H., ZHOU X., TIAN Y., LIN C., WANG W., ZHOU K., ZHANG Y., LIN H. Microplastic abundance, distribution and composition in the mid-west Pacific Ocean. Environmental Pollution. **264**, 114125, **2020**.
16. HAN M., NIU X., TANG M., ZHANG B.T., WANG G., YUE W., KONG X., ZHU J. Distribution of microplastics in surface water of the lower Yellow River near estuary. Science of the Total Environment. **707**, 135601, **2020**.
17. DOMENECH J., MARCOS R. Pathways of human exposure to microplastics, and estimation of the total burden. Current Opinion in Food Science. **42**, 144, **2021**.
18. TANG S., GAO L., GAO H., CHEN Z., ZOU D. Microplastics pollution in China water ecosystems: a review of the abundance, characteristics, fate, risk and removal. Water Science and Technology. **82** (8), 1495, **2020**.
19. ZHANG Y., ZHOU G., YUE J., XING X., YANG Z., WANG X., WANG Q., ZHANG J. Enhanced removal of polyethylene terephthalate microplastics through polyaluminum chloride coagulation with three typical coagulant aids. Science of the Total Environment. **800**, 149589, **2021**.
20. GAO Q., LU X., LI J., WANG P., LI M. Impact of microplastics on nicosulfuron accumulation and bacteria community in soil-earthworms system. Journal of Hazardous Materials. **465**, 133414, **2024**.
21. PADERVAND M., LICHTFOUSE E., ROBERT D., WANG C.Y. Removal of microplastics from the environment. A review. Environmental Chemistry Letters. **18** (3), 807, **2020**.
22. EYDI GABRABAD M., YARI M., BONYADI Z. Using Spirulina platensis as a natural biocoagulant for polystyrene removal from aqueous medium: performance, optimization, and modeling. Scientific Reports. **14** (1), 2506, **2024**.
23. EGEA-CORBACHO A., MARTÍN-GARCÍA A.P., FRANCO A.A., QUIROGA J.M., ANDREASEN R.R., JORGENSEN M.K., CHRISTENSEN M.L. Occurrence, identification and removal of microplastics in a wastewater treatment plant compared to an advanced MBR technology: Full-scale pilot plant. Journal of Environmental Chemical Engineering. **11** (3), 109644, **2023**.
24. FARAHBAKHSH J., GOLGOLI M., KHIADANI M., RAZMJOU A., ZARGAR M. Microplastics fouling mitigation in forward osmosis membranes by the molecular assembly of sulfobetaine zwitterion. Desalination. **575**, 117300, **2024**.
25. DALU T., THEMBA N.N., DONDOFEMA F., CUTHBERT R.N. Nowhere to go! Microplastic abundances in freshwater fishes living near wastewater plants. Environmental Toxicology and Pharmacology. **101**, 104210, **2023**.
26. CAO Z.Q., XIA W., WU S.L., MA J.L., ZHOU X.L., QIAN X.J., XU A.M., DONG W.L., JIANG M. Bioengineering CNB-1: a robust whole-cell biocatalyst for efficient PET microplastic degradation. Bioresources and Bioprocessing. **10** (1), **2023**.
27. SENATHIRAJAH K., KANDAIAH R., PANNEERSELVAN L., SATHISH C.I., PALANISAMI T. Fate and transformation of microplastics due to electrocoagulation treatment: Impacts of polymer type and shape. Environmental Pollution. **334**, 122159, **2023**.
28. ZHOU D.W., LUO H.X., ZHANG F.Z., WU J., YANG J.P., WANG H.P. Efficient Photocatalytic Degradation of the Persistent PET Fiber-Based Microplastics over Pt Nanoparticles Decorated N-Doped TiO_2 Nanoflowers. Advanced Fiber Materials. **4** (5), 1094, **2022**.
29. LIU Y.Z., LI B., LI R.L., JI H.D., SONG L., ZHU X.S., JING L., LIU X.N., HUANG Y.F., WU X.F. Simultaneous removal of microplastics and doxycycline and preparation of novel hollow carbon nanocakes by pyrolysis. Chemical Engineering Journal. **472**, 144999, **2023**.
30. GIRISH N., PARASHAR N., HAIT S. Coagulative removal of microplastics from aqueous matrices: Recent progresses and future perspectives. Science of the Total Environment. **899**, 165723, **2023**.
31. WANG M., HUANG Z., WU C., YAN S., FANG H.T., PAN W., TAN Q.G., PAN K., JI R., YANG L., PAN B., WANG P., MIAO A.J. Stimulated Raman Scattering Microscopy Reveals Bioaccumulation of Small Microplastics in Protozoa from Natural Waters. Environmental Science & Technology. **58** (6), 2922, **2024**.
32. LI Y., ZHEN D., LIU F., ZHANG X., GAO Z., WANG J. Adsorption of azoxystrobin and pyraclostrobin onto degradable and non-degradable microplastics: Performance and mechanism. Science of the Total Environment. **912**, 169453, **2024**.
33. ZHAO J., WANG A., WEI L., GE W., CHI Y., LAI Y. Effect of kaolin on floc properties for reactive orange removal in continuous coagulation process. Water Science and Technology. **78** (3-4), 571, **2018**.
34. ZHANG Y.T., ZHAO J.H., LIU Z.Y., TIAN S.F., LU J.F., MU R., YUAN H.Y. Coagulation removal of microplastics

from wastewater by magnetic magnesium hydroxide and PAM. Journal of Water Process Engineering. **43**, 102250, **2021**.
35. MA B., XUE W., DING Y., HU C., LIU H., QU J. Removal characteristics of microplastics by Fe-based coagulants during drinking water treatment. Journal of Environmental Sciences (China). **78**, 267, **2019**.
36. WEI L., ZHAO J., XU C., LIU M. Experimental analysis of magnesium hydroxide-reactive orange floc formation time and rate in coagulation process. Journal of the Taiwan Institute of Chemical Engineers. **45** (5), 2605, **2014**.
37. YOUNG P., PHASEY J., WALLIS I., VANDAMME D., FALLOWFIELD H. Autoflocculation of microalgae, via magnesium hydroxide precipitation, in a high rate algal pond treating municipal wastewater in the South Australian Riverland. Algal Research. **59**, 102418, **2021**.
38. ZHOU J., YANG Y., LI Z. Efficient and fast arsenate removal from water by in-situ formed magnesium hydroxide. Scientific Reports. **14** (1), 21232, **2024**.
39. ZHANG Y., ZHAO J., LI W., YUAN H. Coagulation properties of magnetic magnesium hydroxide for removal of microplastics in the presence of kaolin and humic acid. Environmental Technology. **45** (8), 1459, **2024**.
40. ZHAO J., SHI H., LIU M., LU J., LI W. Coagulation-adsorption of reactive orange from aqueous solution by freshly formed magnesium hydroxide: mixing time and mechanistic study. Water Science and Technology. **75** (7-8), 1776, **2017**.
41. LI B., ZHAO J.H., GE W.Q., LI W.P., YUAN H.Y. Coagulation-flocculation performance and floc properties for microplastics removal by magnesium hydroxide and PAM. Journal of Environmental Chemical Engineering. **10** (2), 107263, **2022**.